

Stochastic features of dissipative large-amplitude dynamics and nuclear fission

V. M. Kolomietz and S. V. Radionov

Institute for Nuclear Research, 03680 Kiev, Ukraine

(Dated: November 24, 2021)

Abstract

Within a density matrix approach for nuclear many-body system, it is derived non-Markovian Langevin equations of motion for nuclear collective parameters, where memory effects are defined by memory time. The developed stochastic approach is applied to study both the nuclear descent from fission barrier to a scission point and thermal diffusive overcoming of the barrier. The present paper is partly a review of our results obtained earlier and contains new results on the non-Markovian generalization of Kramers' theory of escape rate and on time features of the collective dynamics in the presence of periodic external modulation.

arXiv:2111.02487v2 [nucl-th] 23 Nov 2021

I. INTRODUCTION

Nuclear large-scale dynamics (nuclear fission, heavy ion collisions etc.) is a good probe for the investigation of the complex time evolution of finite Fermi systems. The principal question here is how macroscopic (collective) modes of motion [1–3] are affected by complex microscopic (intrinsic) excitations of the many-body Fermi systems. Due to dissipative and fluctuating character of the collective modes of motion, manifesting in non-zero widths of the nuclear giant multipole resonances and non-zero variances of the kinetic energy of the nuclear fission fragments, one uses transport approaches of the Fokker–Planck and Langevin types [4–11] to the study of nuclear large-amplitude dynamics. In general, basic equations for the macroscopic collective variables are non-Markovian [12, 13], implying complex energy flow between the slow collective and fast intrinsic degrees of freedom of the nuclear many-body system.

In the present paper, following the ideology of the random matrix theory [14, 15] we discuss how non-Markovian (memory) and stochastic aspects of the nuclear fission dynamics are defined by quantum-mechanical diffusion of energy in the space of occupancies of complex many-body states. The general problem of decay of a metastable state (like a decay of nuclear compound state) has gotten a lot of attention in the functional integral approach [16, 17] and in its application to the nuclear case [18]. Quantum decay rate of the nuclear compound state has been derived within the local harmonic approximation [19], where also non-Markovian effects were considered. In spite of such wide literature on the subject, the problem of classical activated (escape) rate over the nuclear fission barrier in the presence of the non-Markovian effects has been left without appropriate attention. We are going to renew this deficiency by measuring a general quantitative impact of memory effects on the classical thermal rate and time characteristics of the nuclear fission dynamics.

The plan of the paper is as follows. In Sect. II, we consider a many-body dynamics by use the Zwanzig’s projection technique and derive the basic non-Markovian Langevin equations of motion within the cranking approach to nuclear many-body dynamics. In Sect. III, we discuss the application of non-Markovian dynamics to the nuclear descent from the fission barrier, the memory effect on the Kramers’ diffusion over the fission barrier, the stochastic penetration over oscillating barrier and the diffusion of occupation probabilities within Landau-Zener approach. The non-Markovian dynamics of nuclear Fermi liquid is

considered in Sect. IV. Summary and conclusions are given in Sect. V.

II. MANY-BODY DYNAMICS IN A MOVING FRAME

We assume that dynamics of nuclear many-body system can be described as a coupled motion of several slow macroscopic (collective) modes and intrinsic nucleonic ones. Slow collective modes are treated in terms of a set of classical time-dependent variables $q(t) \equiv \{q_1(t), q_2(t), \dots, q_N(t)\}$. The fast intrinsic modes are described quantum mechanically through the Liouville equation for the density matrix operator $\hat{\rho}$,

$$\frac{\partial \hat{\rho}(t)}{\partial t} + i\hat{L}(t)\hat{\rho}(t) = 0, \quad (1)$$

where \hat{L} is the Liouville operator defined as

$$\hat{L}\hat{\rho} = \frac{1}{\hbar} [\hat{H}, \hat{\rho}]. \quad (2)$$

Here $\hat{H}(q)$ is the nuclear many-body Hamiltonian. We introduce a moving (adiabatic) basis of the Hamiltonian $\hat{H}(q)$,

$$\hat{H}(q)\Psi_n(q) = E_n(q)\Psi_n(q), \quad (3)$$

determined by a set of eigenfunctions $\Psi_n(q)$ and eigenenergies $E_n(q)$ for each fixed value of the macroscopic variables $q(t)$. Within this basis one can introduce a non-diagonal, ρ_{nm} , and diagonal, ρ_{nn} , parts of the density matrix through the relations,

$$\rho_{nn} = \langle \Psi_n | \hat{\rho} | \Psi_n \rangle, \quad \rho_{nm} = \langle \Psi_n | \hat{\rho} | \Psi_m \rangle, \quad (4)$$

and whose time evolution may be determined within the Zwanzig's projection technique [20]. The final results read, see Refs. [8, 21],

$$\begin{aligned} \rho_{nm}(t) = \rho_{nm}(t=0) - i \sum_{j=1}^N \int_0^t dt' \dot{q}_j(t') \frac{\exp[-i\omega_{nm}(t-t')]}{\omega_{nm}} \\ \times [h_{j,mn}(t')\rho_{nn}(t') - h_{j,nm}(t')\rho_{mm}(t')], \end{aligned} \quad (5)$$

and its diagonal part,

$$\begin{aligned} \frac{\partial \rho_{nn}(t)}{\partial t} = \frac{2}{\hbar^2} \sum_{i,j=1}^N \dot{q}_i(t) \int_0^t dt' \dot{q}_j(t') \sum_{m \neq n} h_{i,nm}(t) h_{j,mn}(t') \frac{\cos[\omega_{nm}(t-t')]}{\omega_{nm}^2} \\ \times [\rho_{mm}(t') - \rho_{nn}(t')]. \end{aligned} \quad (6)$$

Here, $\omega_{nm} = (E_n - E_m)/\hbar$ and matrix elements $h_{i,nm} = \left(\partial\hat{H}/\partial q_i\right)_{nm}$ measure the coupling between the quantum nucleonic and the macroscopic collective subsystems. Note that the equations (5) and (6) were derived in the weak-coupling limit [21]. This condition can be violated near the avoided crossings of two nearest levels. One can go beyond the second-order perturbation result (5)–(6) by considering the Landau–Zener model of two crossing levels as shall be done below.

A complexity of a quantum system is understood as the absence of any special symmetries in a system. Such a system is expected to have some universal statistical properties which can be modeled by the random matrix ensembles. Within the random matrix approach [22], we will average the right-hand side of master equation (6) over suitably chosen statistics of the randomly distributed matrix elements $h_{i,nm}$ and the energy spacings $E_n - E_m$. First, we perform the ensemble averaging over the matrix elements. They are treated as complex random numbers with the real and the imaginary parts which are independently Gaussian distributed, and with [23]

$$\overline{h_{i,nm}(q)h_{j,n'm'}^*(q')} = \delta_{nn'}\delta_{mm'}\sigma_{ij}^2(E_n, E_m, q + q')Y_{ij}(|q - q'|), \quad (7)$$

where $Y_{ij}(|q - q'|)$ is a correlation function, measuring how strong the ensemble averaged matrix elements correlate at different collective deformations q and q' , and $\sigma_{ij}^2(E_n, E_m, q + q')$ is the energy distribution of the squared matrix elements. It is rather clear that at high excitation energies the coupling matrix elements between the complex many-body states should drop out with increasing energy distance between them. In order to characterize the energy distribution of the matrix elements, we introduce the strength of the distribution $\sigma_{0,ij}^2$ and its width Γ_{ij} assuming

$$\sigma_{ij}^2(E_n, E_m, q + q') = \frac{\sigma_{0,ij}^2(E_n + E_m, q + q')}{\sqrt{\Omega(E_n)\Omega(E_m)}\Gamma_{ij}} f_{ij}(|E_n - E_m|/\Gamma_{ij}), \quad (8)$$

where $\Omega(E)$ is the average level-density at given excitation energy E and $f(E)$ is a shape of the energy distribution. The correlations of the matrix elements, existing at different values of the macroscopic parameter, q and q' , are measured with the help of the correlation function Y_{ij} . Since the energy correlations between two different states n and m drop out with the rise of a distance between them, it is rather obvious that $f_{ij} \rightarrow 0$ with $|E_n - E_m|/\Gamma_{ij} \rightarrow \infty$ and $f_{ij}(E) \sim 1$ at $|E_n - E_m|/\Gamma \ll 1$. As is discussed in Refs. [24, 25], for nuclear shell-model Hamiltonians typical values of the spreading width Γ are of several (tens) MeV.

The energy spacings part of the ensemble averaging procedure is defined through the two-level correlation function, $R(|E_n - E_m|\Omega(E))$, that is the probability density to find the state m with energy E_m within the interval $[E_m, E_m + dE_m]$ at the average distance $|E_n - E_m|$ from the given state n with energy E_n . In the case of quite dense spectrum of the adiabatic states n , it is more convenient to use continuous energy variables E and e , that measure a total excitation and distances between different states, correspondingly,

$$E \equiv E_n, \quad e \equiv E_n - E_m, \quad (9)$$

In this variables, the basic equation (6) for the occupancies $\bar{\rho}(E, t)$ of adiabatic states is transformed as

$$\Omega(E) \frac{\partial \bar{\rho}(E, t)}{\partial t} = \sum_{i,j=1}^N \dot{q}_i(t) \int_0^t dt' K_{ij}(t, t') \dot{q}_j(t') \frac{\partial}{\partial E} \left[\Omega(E) \frac{\partial \bar{\rho}(E, t')}{\partial E} \right]. \quad (10)$$

In Eq. (10), the memory kernel, $K_{ij}(t, t')$, is defined as

$$K_{ij}(t, t') = \frac{\sigma_{0,ij}^2(E, q + q')}{\Gamma_{ij}} Y_{ij}(|q - q'|) \int_{-\infty}^{+\infty} de f_{ij}(|e|/\Gamma_{ij}) R[|e|\Omega(E)] \cos(e[t - t']/\hbar). \quad (11)$$

The integration limits over the energy spacing e in Eq. (11) were extended to infinities since the time changes of the occupancy $\bar{\rho}(E, t)$ of the given state with the energy E are mainly due to the direct interlevel transitions from the close-lying states located at the distances $|e| \ll E$. The explicit form of the two-level correlation function $R(x)$ in Eq. (11) depends on the statistical ensemble of levels [26]. It can be established the following result for three often used ensembles:

(i) Gaussian Orthogonal Ensemble (GOE)

$$R_{\text{GOE}}(x) = 1 - \left(\frac{\sin(\pi x)}{\pi x} \right)^2 + \left(\int_0^1 dy \frac{\sin(\pi xy)}{y} - \frac{\pi}{2} \right) \left(\frac{\cos(\pi x)}{\pi x} - \frac{\sin(\pi x)}{(\pi x)^2} \right), \quad (12)$$

(ii) Gaussian Unitary Ensemble (GUE)

$$R_{\text{GUE}}(x) = 1 - \left(\frac{\sin(\pi x)}{\pi x} \right)^2, \quad (13)$$

(iii) Gaussian Symplectic Ensemble (GSE)

$$R_{\text{GSE}}(x) = 1 - \left(\frac{\sin(2\pi x)}{2\pi x} \right)^2 + \int_0^1 dy \frac{\sin(2\pi xy)}{y} \left(\frac{\cos(2\pi x)}{2\pi x} - \frac{\sin(2\pi x)}{(2\pi x)^2} \right), \quad (14)$$

where $x \equiv |E_n - E_m|\Omega(E_n)$.

The main difference between the statistics is its behavior of $R(x)$ at small energy spacings x . For the GOE statistics one has the linear repulsion between levels, $R_{\text{GOE}} \sim x$, the GUE statistics implies the quadratic level repulsion, $R_{\text{GUE}} \sim x^2$, while in the GSE case we have $R_{\text{GSE}} \sim x^4$. On the other hand, R_{GOE} , R_{GUE} and R_{GSE} are similar at moderate spacings x , when the spectral correlations between levels consistently disappear, see also Refs. [10, 22].

Note that the dynamic process (10) may be treated as a quantum mechanical diffusion of energy in space of the occupancies of quantum adiabatic states, where a function

$$W(E, t) \equiv \Omega(E)\bar{\rho}(E, t), \quad \int_{E_0}^{+\infty} W(E, t)dE = 1, \quad (15)$$

gives a probability density to find the intrinsic quantum system with an excitation energy lying in the interval $[E, E + dE]$ at the moment of time t . The time features of the non-Markovian quantum diffusive dynamics (10)–(11) are defined by the relationship between characteristic time scales, $\tau_{ij} \sim \hbar/\Gamma_{ij}$ (caused by the finite width Γ_{ij} of the coupling matrix elements' energy distribution $f_{ij}(E)$) and the typical time interval $\tau_{\text{macro},ij}$ of the macroscopic variables' variations. For nuclear many-body Hamiltonians, showing statistical properties, the energy distribution of the Breit–Wigner shape [25], $f_{ij}(|e|/\Gamma_{ij}) = (1/\pi)/(1 + [|e|/\Gamma_{ij}]^2)$. This gives rise to an exponentially decaying with time memory kernel (11) (here we restrict ourselves by the one-dimension case to simplify the notation)

$$K(t, t') = \sigma_0^2(E, q + q') \exp\left(-\frac{|t - t'|}{\tau}\right) \quad (16)$$

with $\tau = \hbar/\Gamma$. If one now assumes that τ is the shortest time scale in a system, one easily obtains the Markovian limit of the quantum diffusion process (10) in terms of the probability density function of the intrinsic quantum system (15). Namely,

$$\frac{\partial W(E, t)}{\partial t} = -\frac{\partial}{\partial E} [r(E, t)W(E, t)] + \frac{\partial^2}{\partial E^2} [D(E, t)W(E, t)], \quad \frac{\hbar}{\Gamma} \ll \tau_{\text{macro}}, \quad (17)$$

where the drift coefficient $r(E, t)$ is equal to

$$r(E, t) = \frac{dD(E, t)}{dE} + \frac{D(E, t)}{\Omega(E)} \frac{d\Omega(E)}{dE} \quad (18)$$

and the diffusion coefficient $D(E, t)$ is given by

$$D(E, t) = (\hbar/\Gamma) \cdot \sigma_0^2(E, q)q^2. \quad (19)$$

The drift term in the diffusion equation (17) leads to parametric excitation of the intrinsic quantum system that becomes possible either due to the energy-dependence of the distribution of the slopes $\sigma_0^2(E)$ in Eq. (19), or due to the average level-density $\Omega(E)$ that grows

with an intrinsic excitation E . The diffusion coefficient $D(E, t)$ (19) depends quadratically on the velocity \dot{q} of the parametric driving as a result of the assumed weak-coupling regime [21]. It should be pointed out that the quantum-mechanical diffusion in space of many-body states' occupancies gets stronger dependence on the velocity of the driving in the case of Landau-Zener transitions between states (see Subsection III E).

A. Energy rate

To obtain equations of motion for the macroscopic collective parameters $q(t)$, we first find the average energy of the many-body system, $\mathcal{E}(t) = \text{Tr}[\hat{H}\{q(t)\}\hat{\rho}(t)]$. Calculating the time change of $\mathcal{E}(t)$, we obtain

$$\frac{d\mathcal{E}(t)}{dt} = \sum_i \dot{q}_i \frac{\partial E_0(q)}{\partial q_i} + \sum_i \dot{q}_i \sum_{nm} \left(\frac{\partial \hat{H}}{\partial q_i} \right)_{mn} \rho_{nm} + \sum_n E_n \frac{\partial \rho_{nn}}{\partial t} + \sum_i \dot{q}_i \sum_n \left(\frac{\partial \hat{H}}{\partial q_i} \right)_{nn} \rho_{nn}. \quad (20)$$

The first term in the right-hand side of Eq. (20) describes a change of the macroscopic potential energy $E_0(q) = E_{\text{pot}}(q)$. The second contribution to the energy rate $d\mathcal{E}/dt$ is defined by the non-diagonal components of the density matrix $\rho_{nm}(t)$. Its time evolution is caused by the virtual transitions among the adiabatic states. Such a term is a microscopic source for the appearance of the macroscopic kinetic energy. To demonstrate that, we write it as

$$\begin{aligned} \left(\frac{d\mathcal{E}}{dt} \right)^{\text{virt}} &\equiv \sum_i \dot{q}_i \sum_{nm} \left(\frac{\partial \hat{H}}{\partial q_i} \right)_{mn} \rho_{nm} \\ &= \sum_i \dot{q}_i(t) \xi_i(t) + 2 \sum_i \dot{q}_i \sum_j \sum_{nm} \int_0^t dt' \mathcal{V}_{ij, nm}(t, t') \dot{q}_j(t') [\rho_{mm}(t') - \rho_{nn}(t')], \end{aligned} \quad (21)$$

where

$$\xi_i(t) = \left(\frac{\partial \hat{H}}{\partial q_i} \right)_{mn} \rho_{nm}(t=0), \quad \mathcal{V}_{ij, nm}(t, t') = h_{i, nm}(t) h_{j, mn}(t') \frac{\cos(\omega_{nm}[t - t'])}{\omega_{nm}}. \quad (22)$$

We formally extend the lower limit of the time integration in Eq. (21) to $-\infty$. In this way, we would like to study stationary dynamics of the complex quantum system, i. e., when the dynamics of the system does not depend on the choice of initial time. It should be pointed

out that this does not imply a loss of any possible memory effects in collective motion. Thus, integrating by parts the time integral in the r.h.s of Eq. (21), one can show that

$$\int_{-\infty}^t dt' \mathcal{V}_{ij, nm}(t, t') \dot{q}_j(t') [\rho_{mm}(t') - \rho_{nn}(t')] \approx \sum_{l=0}^{+\infty} \omega_{nm}^{-(2l+3)} \times \frac{d^{(2l+1)} (\dot{q}_j h_{i, nm} h_{j, mn} [\rho_{mm} - \rho_{nn}])}{dt^{(2l+1)}}. \quad (23)$$

In the weak-coupling limit [21], we obtain

$$\left(\frac{d\mathcal{E}}{dt} \right)^{\text{virt}} \approx \sum_i \dot{q}_i(t) \xi_i(t) + \sum_i \dot{q}_i \sum_j (B_{ij}(q) \ddot{q}_j + \sum_k \frac{\partial B_{ij}(q)}{\partial q_k} \dot{q}_j \dot{q}_k), \quad (24)$$

where the term

$$B_{ij}(q) = \sum_{n, m} h_{i, nm} h_{j, mn} \omega_{nm}^{-3} [\rho_{mm} - \rho_{nn}] \quad (25)$$

can be associated with a macroscopic inertia tensor.

The third term on the right-hand side of Eq. (20) is determined by the real transitions between the adiabatic states $\Psi_n(q)$ and it defines how the energy of macroscopic motion is transferred into the energy of the intrinsic excitations of the quantum system:

$$\left(\frac{d\mathcal{E}}{dt} \right)^{\text{real}} = \sum_i \dot{q}_i(t) \sum_j \int_0^t dt' K(t, t') \dot{q}_j(t') \int_{E_0}^{+\infty} dE E \frac{\partial}{\partial E} \left(\Omega(E) \frac{\partial \bar{\rho}(E, t')}{\partial E} \right), \quad (26)$$

where Eq. (10) was used.

The fourth term in the r.h.s of Eq. (20) is given by the distribution of slopes of the adiabatic eigenstates E_n . Within the random matrix model, the negative and positive slopes of the adiabatic states are assumed to be equally distributed. Therefore, under the averaging over all random realizations of the random matrices, modeling the nuclear many body spectrum, one can neglect the contribution from the fourth term in the r.h.s. of Eq. (20).

Rewriting the time change of the average energy of the nuclear many-body system (20) as

$$\begin{aligned} \frac{d\mathcal{E}(t)}{dt} &= \sum_i \dot{q}_i(t) F_i(q, t) \\ &\equiv \sum_i \dot{q}_i(t) \left(\frac{\partial E_{\text{pot}}}{\partial q_i} + \xi_i(t) + \sum_j \left[B_{ij} \ddot{q}_j + \sum_k \frac{\partial B_{ij}}{\partial q_k} \dot{q}_j \dot{q}_k \right] \right) \\ &+ \sum_j \int_0^t dt' K_{ij}(t, t') \dot{q}_j(t') \int_{E_0}^{+\infty} dE \Omega(E) E \frac{\partial}{\partial E} \left[\Omega(E) \frac{\partial \bar{\rho}(E, t')}{\partial E} \right] \end{aligned} \quad (27)$$

and assuming that all the partial contributions $F_i(q, t)$ to the energy rate (having a meaning of the forces acting on the macroscopic collective subsystem) are equal zero, we obtain transport description of the macroscopic collective dynamics

$$\begin{aligned}
& \sum_j \left[B_{ij} \ddot{q}_j + \sum_k \frac{\partial B_{ij}}{\partial q_k} \dot{q}_j \dot{q}_k \right] = - \frac{\partial E_{\text{pot}}}{\partial q_i} \\
& - \sum_j \int_0^t dt' K_{ij}(t, t') \dot{q}_j(t') \int_{E_0}^{+\infty} dE E \frac{\partial}{\partial E} \left[\Omega(E) \frac{\partial \bar{\rho}(E, t')}{\partial E} \right] - \xi_i(t).
\end{aligned} \tag{28}$$

B. Fluctuation–dissipation theorem

The transport equations (28) for the classical collective parameters $q(t)$ should be considered selfconsistently with the equation of motion for the occupancies $\bar{\rho}(E, t)$ of the quantum many–body states (10). As was stated above (see Eq. (17) and comment to it), the intrinsic quantum system is excited by time variations of the collective parameters $q(t)$ provided that the averaged density of the many–body states $\Omega(E)$ grows with the excitation E . Importantly that such a parametric excitation is time–irreversible in the sense that the intrinsic quantum system (10) does not go back to the initial state with time–reversing of the macroscopic collective parameters but continues to be excited. This is so because under the parametric time variations (defined by the absolute value of the parameters' velocity $|\dot{q}(t)|$, see Eqs. (18) and (19)), quantum–mechanical transitions to higher–lying states occur more often than to lower–lying states. In turn, due to the energy conservation condition (20), the increase of the intrinsic excitation

$$E^*(t) \equiv \int_{E_0}^{+\infty} dE \Omega(E) E \bar{\rho}(E, t) \tag{29}$$

of the nuclear many–body system may be interpreted as a corresponding decrease (dissipation) of an energy associated with the time variations of the macroscopic collective parameters $q(t)$:

$$E_{\text{coll}} \equiv \sum_{i,j} \frac{1}{2} B_{i,j}(q) \dot{q}_i \dot{q}_j + E_{\text{pot}}(q). \tag{30}$$

In this way, we justified microscopically dissipative character of the nuclear collective motion. For quite high initial excitations of the nucleus $E^*(t = 0)$, when the averaged density of

many-body states is given by

$$\Omega(E^*(t=0)) \sim e^{E^*(t=0)/T}, \quad (31)$$

the collective dissipation is determined by memory kernels

$$\mathcal{K}_{ij}(t, t') = \frac{\sigma_{0,ij}^2(E^*(t=0), q[t] + q[t'])}{T} \exp\left(-\frac{|t-t'|}{\tau_{ij}}\right), \quad (32)$$

of the retarded friction forces in the transport equations of motion

$$\sum_j \left[B_{ij} \ddot{q}_j + \sum_k \frac{\partial B_{ij}}{\partial q_k} \dot{q}_j \dot{q}_k \right] = -\frac{\partial E_{\text{pot}}}{\partial q_i} - \sum_{j,k} \frac{\partial B_{ij}}{\partial q_k} \dot{q}_j \dot{q}_k - \sum_j \int_0^t dt' \mathcal{K}_{ij}(t, t') \dot{q}_j(t') - \xi_i(t), \quad (33)$$

In Eqs. (31)–(33), a quantity T is considered as thermodynamic temperature of the nucleus.

To complete the transport description of the macroscopic collective dynamics (33) one has to define statistical properties of the terms $\xi_i(t)$ (22), which are proportional to the non-diagonal components ρ_{nm} of the density matrix operator $\hat{\rho}(t)$ at initial moment of time $t = 0$. If the initial distribution of the diagonal components ρ_{nn} is uniquely set in by the initial excitation energy of the nuclear many-body system $E^*(t=0)$ (29), the initial values of the non-diagonal components ρ_{nm} are left without specifying. For each fixed value of the initial excitation $E^*(t=0)$, one has a bunch of the values $\rho_{nm}(t=0)$ which may be treated as random numbers. In this case, we can treat the terms $\xi_i(t)$ in the transport equations (33) as random forces acting on the macroscopic collective parameters $q_i(t)$, $i = 1, 2, \dots$. By using Eqs. (22),(7) and (32), we obtain for correlation functions of the random forces $\xi_i(t)$,

$$\langle \xi_i(t) \xi_j(t') \rangle = T \mathcal{K}_{ij}(t, t'), \quad (34)$$

where it was assumed for simplicity that $|\rho_{nm}(t=0)|^2 = 1$. The result (34) represents the classical fluctuation-dissipation relation between dissipative and fluctuating properties of the macroscopic collective dynamics both caused by the quantum-mechanical diffusion of energy in the space of the occupancies of many-body states (10).

III. APPLICATION TO LARGE-AMPLITUDE COLLECTIVE MOTION

A. Descent from the fission barrier

We are going to apply the developed transport approach (33)–(34) to the nuclear fission in two dimension space of shape variables $\{q_1, q_2\}$. We consider the symmetric fission of

heavy nuclei whose shape is obtained by rotation of a profile function $\mathcal{L}(z)$ around z -axis. The Lorentz parameterization for $\mathcal{L}(z)$ is used in the following form [2],

$$\mathcal{L}^2(z) = (z^2 - \zeta_0^2)(z^2 + \zeta_2^2)/Q, \quad (35)$$

where the multiplier Q guarantees the volume conservation,

$$Q = -[\zeta_0^3(\frac{1}{5}\zeta_0^2 + \zeta_2^2)]/R_0^3. \quad (36)$$

Here, all quantities of the length dimension are expressed in the R_0 units, where R_0 is the radius of equal-sized sphere. The shape variables $q_1 = \zeta_0$ and $q_2 = \zeta_2$ are related to the nuclear elongation, ζ_0 , and the neck radius $\rho_{\text{neck}} = \zeta_2/\sqrt{\zeta_0(\zeta_0^2/5 + \zeta_2^2)}$. The basic equations of motion (33) in two dimensions is written as

$$\sum_{j=1}^2 \left[B_{ij}(q)\ddot{q}_j + \sum_{k=1}^2 \frac{\partial B_{ij}(q)}{\partial q_k} \dot{q}_j \dot{q}_k \right] = -\frac{\partial E_{\text{pot}}(q)}{\partial q_i} - \sum_{j=1}^2 \int_0^t dt' \mathcal{K}_{ij}(t, t') \dot{q}_j(t') - \xi_i(t). \quad (37)$$

The numerical calculations are performed for the symmetric fission of the nucleus ^{236}U at temperature $T = 2$ MeV. Considering the nuclear descent from the saddle point to the scission, we use the potential energy of deformation $E_{\text{pot}}(\zeta_0)$ from Ref. [2] assuming that $\partial E_{\text{pot}}(q_1, q_2)/\partial \rho_{\text{neck}} = 0$. The scission line is derived from the condition of the instability of the nuclear shape with respect to any variations of the neck radius:

$$\left. \frac{\partial^2 E_{\text{pot}}(q_1, q_2)}{\partial \rho_{\text{neck}}^2} \right|_{\text{scis}} = 0 \quad (38)$$

Here, we wish to study the random force effect on the non-Markovian dynamics (37). To define properly a scission condition, we first introduce a deterministic (i. e., without the random force) path of the system (37) and evaluate the nuclear neck radius at the scission point $(\rho_{\text{neck}}^{\text{det}})_{\text{scis}}$. Then, a bunch of 2×10^4 stochastic trajectories $\zeta_0(t), \zeta_2(t)$ is stopped as far as

$$\rho_{\text{neck}}(\zeta_0(t), \zeta_2(t)) = (\rho_{\text{neck}}^{\text{det}})_{\text{scis}}. \quad (39)$$

As a result of that, we get a distribution of moments of time, t_{sc} , when the system reaches the scission point (38). The corresponding probability density p of the scission events is shown in figure 1 for the case of quite weak memory effects $\tau_1 = 2 \times 10^{-23}$ s and fairly strong memory effects $\tau_2 = 8 \times 10^{-23}$ s. For comparison, it is also shown (by vertical lines) the corresponding scission times in the absence of the random force.

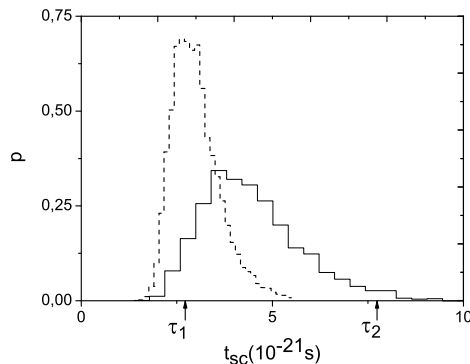


FIG. 1: Histogram, showing a probability density p of moments of time t_{sc} , when the stochastic trajectories $\zeta_0(t), \zeta_2(t)$ (37) hit the scission line $\rho_{\text{neck}}(\zeta_0, \zeta_2) = (\rho_{\text{neck}}^{\text{det}})_{\text{scis}}$, is given at two values of the memory time τ . The dashed histogram is found for $\tau_1 = 2 \times 10^{-23}$ s (when the memory effects in the system are quite weak) and the solid histogram corresponds to the memory time $\tau_2 = 8 \times 10^{-23}$ s (when the memory effects are fairly strong). The corresponding times of descent in the absence of the random force are given by small vertical arrows. Taken from Ref. [11].

We see that with the growth of the memory effects in (37) the distribution of the scission times t_{sc} becomes wider and the centroid of the distribution shifts to the left compared to the deterministic values of the scission time. One can interpret this as a "stochastic" acceleration of the nuclear descent from fission barrier, caused by the presence of the random force term in equations of motion (37), see also Ref. [11].

Note that within the two-dimensional non-Markovian Langevin approach (37)–(38) one can also calculate other characteristics of nuclear fission process. Thus, in Ref. [11] we have calculated two experimentally observable quantities like the mean value and variance of the total kinetic energy of fission fragments at infinity. By that, we have estimated the value of memory time and found that $\tau \approx 8 \times 10^{-23}$ s.

B. Escape rate problem within the Langevin approach

To measure the role of memory effects in collective dynamics of the nuclear system on the way from ground state to saddle point, we restrict ourselves by considering a one-dimensional collective motion $q(t)$ over a schematic parabolic barrier shown in figure 2. The potential energy E_{pot} presents a single-well barrier formed by a smoothing joining at $q = q^*$

of the potential minimum oscillator with the inverted oscillator [3]

$$E_{\text{pot}} = \begin{cases} \frac{1}{2}B\omega_A^2(q - q_A)^2, & q \leq q^*, \\ = E_{\text{pot,B}} - \frac{1}{2}B\omega_B^2(q - q_B)^2, & q > q^*. \end{cases} \quad (40)$$

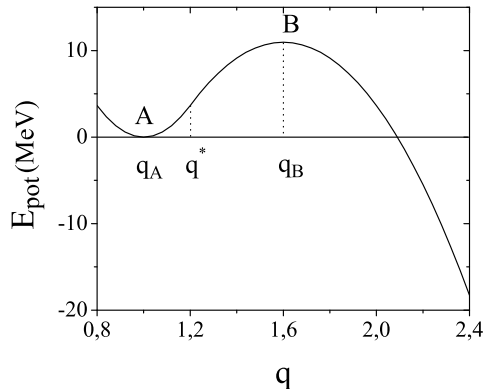


FIG. 2: Dependence of the potential energy E_{pot} (Kramers' potential) on the shape parameter q .

We also adopt constant value B for the collective inertia tensor (25) and for the energy distribution σ_0^2 of the coupling matrix elements in (32), leading us to the equation of motion for the collective variable $q(t)$,

$$B\ddot{q} = -\frac{\partial E_{\text{pot}}}{\partial q} - \mathcal{K}_0 \int_0^t dt' \exp\left(-\frac{|t-t'|}{\tau}\right) \dot{q}(t') - \xi(t), \quad (41)$$

where $\mathcal{K}_0 = \sigma_0^2/T$ and

$$\langle \xi(t)\xi(t') \rangle = T\mathcal{K}_0 \exp\left(-\frac{|t-t'|}{\tau}\right), \quad (42)$$

see Eq. (34).

We studied the non-Markovian Langevin dynamics (41), (42) by calculating a distribution of times $t_{\text{pre-sad}}$ of the first crossing of the barrier top (pre-saddle times). For that, the equation of motion (41) is solved numerically by generating a bunch of the trajectories, all starting at the potential well (point A in figure 2) and having the initial velocities distributed according to the Maxwell-Boltzman distribution. On left panel of figure 3, it is shown the mean pre-saddle time $\langle t_{\text{pre-sad}} \rangle$ as a function of the memory time τ and right panel of figure 3 gives the ration between the standard deviation $\sigma(t_{\text{pre-sad}})$ and the mean value $\langle t_{\text{pre-sad}} \rangle$ of the pre-saddle time distribution.

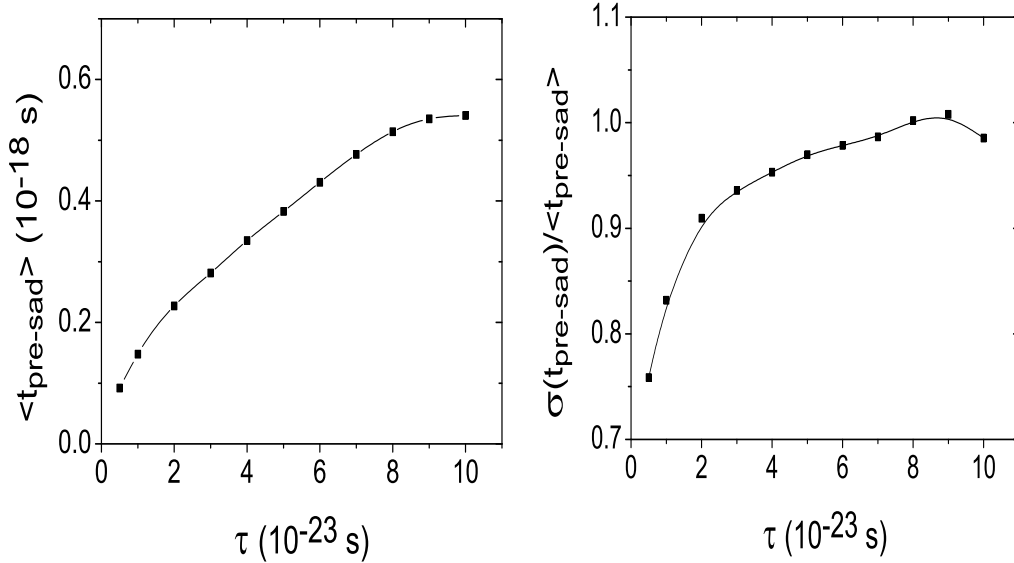


FIG. 3: The mean pre-saddle time $\langle t_{\text{pre-sad}} \rangle$ (left panel) and the standard deviation $\sigma(t_{\text{pre-sad}})$ over $\langle t_{\text{pre-sad}} \rangle$ (right panel) of the non-Markovian diffusion dynamics (41), (42) are shown as a function of the memory time τ .

An increase of the mean time $\langle t_{\text{pre-sad}} \rangle$ of motion from the potential minimum q_A to the saddle point q_B with the memory time τ means that the memory effects in the Langevin dynamics (41),(42) hinders the diffusion over barrier. With growth of the memory time τ the adiabatic conservative force $-(\partial E_{\text{pot}}/\partial q)$ in equation of motion (41) gets an additional contribution from the time-retarded force

$$-\mathcal{K}_0 \int_0^t \exp\left(-\frac{|t-t'|}{\tau}\right) \dot{q}(t') dt' \rightarrow -\mathcal{K}_0 [q(t) - q_A], \quad \omega_B \tau \rightarrow \infty, \quad (43)$$

leading to the subsequent slowing down of motion to the saddle point q_b . In the opposite limit of quite small values of the memory time τ , the slowing down of motion is exclusively due to effect from an usual friction force since

$$-\mathcal{K}_0 \int_0^t \exp\left(-\frac{|t-t'|}{\tau}\right) \dot{q}(t') dt' \rightarrow -\mathcal{K}_0 \tau \dot{q}(t), \quad \omega_B \tau \rightarrow 0. \quad (44)$$

Also note that with the growth of the memory time τ , the pre-saddle time distribution becomes wider as it is followed from right panel of figure 3.

C. Non-Markovian extension of the Kramers model

One can also study the non-Markovian thermal diffusion over the parabolic barrier (41), (42) with the help of an escape rate characteristics, R_0 , defining an exponential time decay of the probability $\text{Prob}(q[t] < q_B)$,

$$\text{Prob}(q[t] < q_B) = e^{-R_0 t}, \quad t > 1/\gamma_0, \quad (45)$$

that the system $q[t]$ does not still reach the barrier top at q_B . Note that the exponential decay with time of the survival probability (45) is reached at sufficiently large times t , when t is larger than the inverse characteristic friction coefficient γ_0 , that will be derived below.

To get an analytical estimate for the escape rate R_0 , one can naturally try to use the formalism of the Kramers' theory [29] and that must be extended to the non-Markovian system (41),(42). With this purpose, we write down the equation of motion (41) for the collective variable $q(t)$ in the vicinity of the barrier top q_B ,

$$B\ddot{q} = B\omega_B^2(q - q_B) - \mathcal{K}_0 \int_0^t dt' \exp\left(-\frac{|t-t'|}{\tau}\right) \dot{q}(t') - \xi(t). \quad (46)$$

General solution to the integro-differential equation (46) is written as

$$q(t) = q_B + \mathcal{A}(t)q_0 + \mathcal{B}(t)v_0 - \int_0^t \mathcal{B}(t-t')\xi(t') \quad (47)$$

or, in terms of velocity

$$v(t) = \dot{\mathcal{A}}(t)q_0 + \dot{\mathcal{B}}(t)v_0 - \int_0^t \dot{\mathcal{B}}(t-t')\xi(t')dt', \quad (48)$$

where q_0 is an initial coordinate and v_0 is an initial velocity of the system. Two functions $\mathcal{A}(t)$ and $\mathcal{B}(t)$ are given by

$$\mathcal{A}(t) = 1 + \omega_B^2 \int_0^t \mathcal{B}(t')dt', \quad \mathcal{B}(t) = D_1 e^{s_1 t} + D_2 e^{s_2 t} + D_3 e^{s_3 t}, \quad (49)$$

where s_1, s_2 and s_3 are roots of the secular equation

$$s^3 + \frac{1}{\tau}s^2 + \frac{\mathcal{K}_0 - \omega_B^2}{B}s - \frac{\omega_B^2}{B\tau} = 0 \quad (50)$$

and the coefficients D_1, D_2 and D_3 equal to

$$D_1 = \frac{(s_1 + 1/\tau)}{(s_1 - s_2)(s_1 - s_3)}, \quad D_2 = \frac{-(s_2 + 1/\tau)}{(s_1 - s_2)(s_2 - s_3)}, \quad D_3 = \frac{(s_3 + 1/\tau)}{(s_1 - s_3)(s_2 - s_3)}. \quad (51)$$

The solutions to the secular equation (50) have a threshold behavior. For small enough memory times $\tau < \tau_{\text{thresh}}$ (weak memory effects in the equation of motion (46), the first root s_1 of the secular equation (50) is a positive number, while the other two roots s_2 and s_3 are negative ones. In this case, the mean collective path $\langle q(t) \rangle$ becomes to grow exponentially with time as

$$\langle q(t) \rangle = a_1 \exp(s_1 t) + a_2 \exp(-|s_2|t) + a_3 \exp(-|s_3|t). \quad (52)$$

In the case of fairly large memory times $\tau > \tau_{\text{thresh}}$ (strong enough memory effects), s_1 is still a positive number, whereas s_2 and s_3 become complex conjugated numbers, that results in appearing of characteristic time oscillations of $\langle q(t) \rangle$:

$$\langle q(t) \rangle = a_1 \exp(s_1 t) + a_4 \exp(-|\text{Im}[s_2]|t) \sin(\text{Re}[s_2]t) + a_5 \exp(-|\text{Im}[s_2]|t) \cos(\text{Re}[s_2]t). \quad (53)$$

Since the random force $\xi(t)$ is Gaussian (but non-Markovian because of Eq. (42)), the two-dimensional process $\{q(t), v(t)\}$ (47)–(48) is also Gaussian and is defined by the probability distribution function [36],

$$\begin{aligned} \mathcal{W}(q \equiv q - q_B, q_0; v, v_0; t) &= \frac{1}{2\pi\sigma_q(t)\sigma_v(t)\sqrt{1-r_{qv}(t)}} \\ &\times \exp\left(-\frac{1}{2(1-r_{qv}^2(t))} \left\{ \frac{[q - \langle q(t) \rangle]^2}{\sigma_q^2(t)} + \frac{[v - \langle v(t) \rangle]^2}{\sigma_v^2(t)} - \frac{2r_{qv}(t)[q - \langle q(t) \rangle][v - \langle v(t) \rangle]}{\sigma_q(t)\sigma_v(t)} \right\}\right), \end{aligned} \quad (54)$$

where

$$\sigma_q(t) = \sqrt{\langle q^2(t) \rangle - \langle q(t) \rangle^2}, \quad \sigma_v(t) = \sqrt{\langle v^2(t) \rangle - \langle v(t) \rangle^2}, \quad r_{qv}(t) = \langle q(t)v(t) \rangle. \quad (56)$$

All the time-dependent functions in (55) can be expressed in terms of the functions $\mathcal{A}(t)$ and $\mathcal{B}(t)$ (49) through the relations (47)–(49) and (42). Knowing the probability distribution function $\mathcal{W}(q, q_0; v, v_0; t)$, one can obtain the corresponding Fokker–Planck equation. We omit several intermediate steps in deriving of the Fokker–Planck equation (for details, see e.g. Ref. [37]) and give the final result

$$\begin{aligned} \left[\frac{\partial}{\partial t} + v \frac{\partial}{\partial q} + \tilde{\omega}_B^2(t) q \frac{\partial}{\partial v} \right] \mathcal{W}(q \equiv q - q_B, q_0; v, v_0; t) &= \frac{\gamma(t)}{B} \frac{\partial}{\partial v} [v \mathcal{W}] \\ &+ \frac{T\gamma(t)}{B^2} \frac{\partial^2 \mathcal{W}}{\partial v^2} + \frac{T}{B\omega_B^2} [\tilde{\omega}_B^2(t) - \omega_B^2] \frac{\partial^2 \mathcal{W}}{\partial v \partial q}. \end{aligned} \quad (57)$$

Here, the time–dependent friction coefficient $\gamma(t)$ and the renormalized frequency parameter $\tilde{\omega}_B(t)$ of the parabolic potential barrier are given by

$$\gamma(t) = B \frac{\ddot{\mathcal{A}}(t)\mathcal{B}(t) - \mathcal{A}(t)\ddot{\mathcal{B}}(t)}{\mathcal{A}(t)\dot{\mathcal{B}}(t) - \dot{\mathcal{A}}(t)\mathcal{B}(t)}, \quad \tilde{\omega}_B^2(t) = \frac{\dot{\mathcal{A}}(t)\ddot{\mathcal{B}}(t) - \ddot{\mathcal{A}}(t)\dot{\mathcal{B}}(t)}{\mathcal{A}(t)\dot{\mathcal{B}}(t) - \dot{\mathcal{A}}(t)\mathcal{B}(t)}. \quad (58)$$

The non–Markovian character of the system shows up in the time–dependence of the friction coefficient γ and frequency parameter $\tilde{\omega}_B^2$, and in the presence of a cross–term $\sim \partial^2\mathcal{W}/\partial v\partial q$. The Markovian limit of the Fokker–Planck equation (57) is reached at $\omega_B\tau \rightarrow 0$, when the retarded force in Eq. (46) simply turns to an ordinary friction force (44). In general case, of course, the retarded force contains both the time–dependent friction and conservative contributions,

$$- \mathcal{K}_0 \int_0^t \exp\left(-\frac{|t-t'|}{\tau}\right) \dot{q}(t') dt' = -\gamma(t)\dot{q}(t) + B(\tilde{\omega}_B^2(t) - \omega_B^2)(q(t) - q_0). \quad (59)$$

We are looking for the stationary solution to Eq. (57) in the form

$$\mathcal{W}_{\text{stat}}(q; v) = \text{const} \cdot \mathfrak{F}(q, v) \cdot \exp\left(-\frac{Bv^2/2}{T} - \frac{[E_{\text{pot},B} - B\tilde{\omega}_{B,\text{sat}}^2 q^2/2]}{T(1+\epsilon)}\right), \quad (60)$$

where $\epsilon = [\tilde{\omega}_{B,\text{sat}}^2 - \omega_B^2]/\omega_B^2$. Substituting the solution (60) into Eq. (57), we obtain an equation for the function $\mathfrak{F}(q, v)$

$$(1+\epsilon)v \frac{\partial \mathfrak{F}}{\partial q} + \left(\frac{1}{1+\epsilon} \tilde{\omega}_{B,\text{sat}}^2 q + \frac{\gamma_0 v}{B}\right) \frac{\partial \mathfrak{F}}{\partial v} = \frac{T\gamma_0}{B^2} \frac{\partial^2 \mathfrak{F}}{\partial v^2} + \frac{T\epsilon}{B} \frac{\partial^2 \mathfrak{F}}{\partial v \partial q}. \quad (61)$$

In Eqs. (60) and (61), γ_0 and $\tilde{\omega}_{B,\text{sat}}^2$ are long time values of the corresponding quantities (58) taken at $\omega_B t \gg 1$. We found that

$$\gamma_0 = -2B(s_1 + \min(s_2, s_3)), \quad \tilde{\omega}_{B,\text{sat}}^2 = -(s_1 - \min(s_2, s_3)), \quad \tau < \tau_{\text{thresh}}. \quad (62)$$

To be precise, at $\tau > \tau_{\text{thresh}}$ the quantities γ_0 and $\tilde{\omega}_{B,\text{sat}}^2$ do not exist as far as the friction coefficient $\gamma(t)$ and frequency parameter $\tilde{\omega}_B^2(t)$ are strongly oscillating functions of time, taking positive as well as negative values. The oscillations of $\gamma(t)$ and $\tilde{\omega}_B^2(t)$ are caused by the structure of functions $\mathcal{A}(t)$ and $\mathcal{B}(t)$, see Eqs. (58) and (49). Formally, we will use the quantities γ_0 and $\tilde{\omega}_{B,\text{sat}}^2$ even in the case of $\tau > \tau_{\text{thresh}}$ in view of the fact that one actually needs not the values γ_0 and $\tilde{\omega}_{B,\text{sat}}^2$ itself but some combination of them, that can be properly defined at the long time $\omega_B t \gg 1$ limit.

Looking now for the solution of Eq. (61) in the form

$$\mathfrak{F} \equiv \mathfrak{F}(v - aq) \equiv \mathfrak{F}(\zeta) \quad (63)$$

and repeating all derivation's steps of the Kramers' theory, we get

$$\mathfrak{F}(\zeta) = \mathfrak{F}_0 \int_{-\infty}^{\zeta} \exp \left[-\frac{\{(1+\epsilon)a - \gamma_0/B\}}{[2T/B]\{\gamma_0/B - \epsilon a\}} \zeta'^2 \right] d\zeta', \quad (64)$$

with

$$\mathfrak{F}_0 = \sqrt{\frac{\{(1+\epsilon)a - \gamma_0/B\}}{[2\pi T/B]\{\gamma_0/B - \epsilon a\}}} \quad (65)$$

and

$$a = \frac{1}{1+\epsilon} \left[\sqrt{\frac{\gamma_0^2}{4B^2} + \tilde{\omega}_{B,\text{sat}}^2} + \frac{\gamma_0}{2B} \right]. \quad (66)$$

Therefore, the escape rate R_0 over parabolic barrier is found as

$$R_0 = \frac{\omega_A}{2\pi\omega_B} \left[\sqrt{\frac{\gamma_0^2}{4B^2} + \tilde{\omega}_{B,\text{sat}}^2} - \frac{\gamma_0}{2B} \right] e^{-E_{\text{pot},B}/T} = \frac{\omega_A}{2\pi\omega_B} s_1 e^{-E_{\text{pot},B}/T} \quad (67)$$

that differs from the standard Kramers' result,

$$R_{\text{Kr}} = \frac{\omega_A}{2\pi\omega_B} \left[\sqrt{\frac{\gamma_0^2}{4B^2} + \omega_B^2} - \frac{\gamma_0}{2B} \right] e^{-E_{\text{pot},B}/T}, \quad (68)$$

by memory effects' modification $\tilde{\omega}_{B,\text{sat}}$ of the frequency parameter ω_B at the top of barrier. We would like to stress that the transition in Eq. (67) from a nonlinear combination of the friction coefficient γ_0 and frequency parameter $\tilde{\omega}_{B,\text{sat}}$ to the largest positive root s_1 of the secular equation (50) is mathematically precise at any size τ of the memory effects, see discussion after Eq. (62).

In figure 4, we show by solid spline-fitting curve the escape rate R_0 derived numerically from the Langevin collective dynamics (41), (42). Analytical estimate of R_0 , given by the non-Markovian extension of the Kramers' rate formula (67) is shown in figure 8 by dashed line. For comparison, we also plotted in figure by dotted line the standard Kramers' expression for the escape rate (68) with the τ -dependent friction coefficient

$$\gamma_0(\tau) = \frac{\mathcal{K}_0\tau}{1 + [\mathcal{K}_0/B]\tau^2}, \quad (69)$$

that correctly covers two limiting situations (44) and (43) of the retarded friction force in Eq. (41).

One can see that the result (67) correctly reproduces the decrease of the rate R of non-Markovian diffusion over barrier with the memory time τ (dashed line). On the other hand, the improved standard Kramers' formula, given by Eqs. (68) and (69), overestimates the

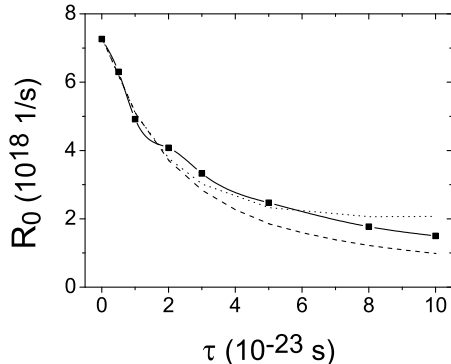


FIG. 4: Escape rate R_0 vs memory time τ . Solid spline-fitting curve represents direct numerical determination of R_0 (45) from the Langevin dynamics Eqs. (41) and (42). Dashed line shows the result of the non-Markovian extension of the Kramers' formula (67). The improved formulation (68)–(69) of the standard Kramers' formula is given by dotted line.

value of R_0 at fairly large memory times τ , see dotted line. From that, one can conclude an importance of the taking into account the memory-renormalization of the stiffness of the system near the top of a potential barrier.

In the discussion above, we did not consider for a quantum tunneling mechanism of the fission barrier penetration. This is justified by the fact that the considered nucleus temperature of 2 MeV is above the characteristic crossover temperature T_0 [16, 17],

$$T_0 = \frac{\hbar s_1}{2\pi}, \quad (70)$$

which defines region where tunneling transitions dominate over thermally activated transitions across the barrier. We found that $T_0 \leq 0.13$ MeV at any value of the memory time τ .

D. Stochastic penetration over oscillating barrier

One of the applications of the stochastic approach to the large amplitude motion is the study of the features of the response of complex nonlinear systems on periodic external field. The very famous example of such features is the stochastic resonance phenomenon [38, 39], when the response of the nonlinear system on the harmonic perturbation is resonantly activated under some optimal level of a noise. The resonant activation of the system occurs

when the frequency of the modulation is near the Kramers' escape rate of the transitions from one potential well to another. The prototype of the stochastic resonance studies is a model of overdamped motion between potential wells of the bistable system. The frequency of the transitions between wells is given by the Kramers' rate and the stochastic resonance is achieved when a frequency of an external periodic modulation is of the order of the Kramers' rate.

We start from the general Langevin formulation (41), (42) of the problem of diffusive overcoming of the potential barrier (40) in the presence of a harmonic time perturbation:

$$B\ddot{q}(t) = -\frac{\partial E_{\text{pot}}}{\partial q} - \mathcal{K}_0 \int_0^t \exp\left(-\frac{|t-t'|}{\tau}\right) \dot{q}(t') dt' - \xi(t) + \alpha \cdot \sin(\omega t), \quad (71)$$

where α and ω are an amplitude and frequency of the perturbation and the correlation function of the random force $\xi(t)$ is given by Eq. (42). Considering the diffusion over the barrier (71),(42) in the presence of the external harmonic force, we assume that the amplitude α of the periodic in time force $\alpha \cdot \sin(\omega t)$ is so small that still the reaching the top of the barrier is caused exclusively by diffusive nature of the process. In figure 5, we show the typical dependencies of the mean pre-saddle time $t_{\text{pre-sad}}$ on the frequency ω of the external harmonic force. The calculations were performed for the weak, $\tau = 2 \times 10^{-23}$ s, (lower curve in figure 5) and strong, $\tau = 10 \times 10^{-23}$ s, (upper curve in figure 5) memory effects in the non-Markovian diffusive motion over barrier.

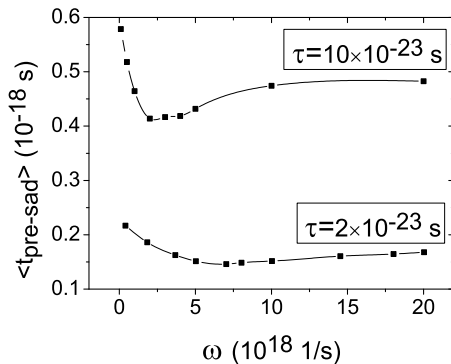


FIG. 5: The mean pre-saddle time $\langle t_{\text{pre-sad}} \rangle$ of the non-Markovian diffusion process (71), (42) is given as a function of the frequency ω of the harmonic time perturbation at two values of the correlation time $\tau = 2 \times 10^{-23}$ s (lower curve) and $\tau = 10 \times 10^{-23}$ s (upper curve).

In both cases the mean pre-saddle time $\langle t_{\text{pre-sad}} \rangle$ non-monotonically depends on the

frequency of the perturbation that is character for the stochastic resonance phenomenon observed in a number of different physical systems. From figure 5 one can conclude that the diffusion over potential barrier in the presence of a harmonic time perturbation is maximally accelerated at some definite so to say resonant frequency ω_{res} of the perturbation,

$$\omega_{\text{res}} \approx \frac{1.5}{\langle t_{\text{pre-sad}} \rangle(\omega = 0)} \quad (72)$$

see also figure 2. In fact, the quantity $\langle t_{\text{pre-sad}} \rangle(\omega = 0)$ presents the characteristic time scale for the diffusion dynamics (71). In the case of adiabatically slow time variations of the harmonic force, $\omega \langle t_{\text{pre-sad}} \rangle(\omega = 0) \ll 1$ and $t < \langle t_{\text{pre-sad}} \rangle$, one can approximately use $\alpha \cdot \sin(\omega t) \approx \alpha \cdot \omega t$ and the diffusion over the barrier is slightly accelerated. As a result of that, the mean pre-saddle time $\langle t_{\text{pre-sad}} \rangle(\omega)$ is smaller than the corresponding unperturbed value $\langle t_{\text{pre-sad}} \rangle(\omega = 0)$. The same feature is also observed at the fairly large modulation's frequencies. Thus, in the case of $\omega \langle t_{\text{pre-sad}} \rangle(\omega = 0) \gg 1$, the harmonic perturbation $\alpha \cdot \sin(\omega t)$ may be treated as a random noise term with the zero mean value and variance α^2 . Such a new stochastic term will lead to additional acceleration of the diffusion over the barrier.

The existence of the resonant regime (72) in the periodically modulated diffusion process (71) is even more clear visible through the time evolution of the survival probability $\text{Prob}(q[t] < q_B)$. For convenience, in figure 6 we plotted $\ln \text{Prob}(q[t] < q_B)$ for the resonant frequency (72) $\omega = \omega_{\text{res}}$ (curve 1), for fairly large frequency $\omega = 10\omega_{\text{res}}$ (curve 2) and for quite small frequency $\omega = \omega_{\text{res}}/10$ (curve 3) of the periodic time modulation.

At very rare ($\omega = \omega_{\text{res}}/10$) or frequent ($\omega = 10\omega_{\text{res}}$) periodic perturbations the probability $\text{Prob}(q[t] < q_B)$ of finding the system $q(t)$ (71) on the left from the saddle point q_B exponentially decay with time and characterized by almost constant escape (decay) rate R_0 , see Eq. (45). On the other hand, periodic modulation of the non-Markovian diffusive dynamics (71), (42) at the resonance frequency $\omega = \omega_{\text{res}}$ provides much stronger decay with time for the survival probability, $\text{Prob}(q[t] < q_B) \sim \exp(-at^2)$. In that case, the probability flow over the saddle point is resonantly amplified.

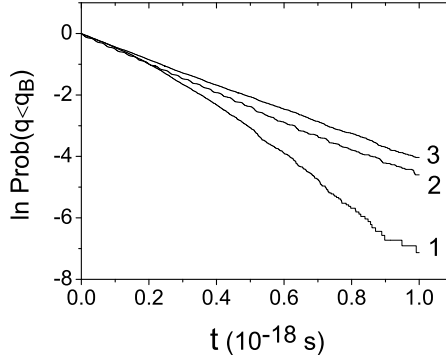


FIG. 6: Natural logarithm of the survival probability $\ln \text{Prob}(q[t] < q_B)$ is given as a function of time t for the periodically modulated escape dynamics (71), (42). Curve 1 corresponds to the modulation on the resonance frequency (72) $\omega = \omega_{\text{res}}$, curve 2 – on the frequency $\omega = 10\omega_{\text{res}}$ and curve 3 – on the frequency $\omega = \omega_{\text{res}}/10$. The time dependencies are calculated for the memory time $\tau = 2 \times 10^{-23}$ s.

E. Diffusion of occupation probabilities within Landau-Zener approach

We restrict our analysis of the Landau-Zener approach to the one-dimensional case and reduce the basic master equation (6). To eliminate the strong time oscillations of the observed quantities $\rho_{nn}(t)$ etc. we introduce the time averaging as

$$\bar{A}(t) = \frac{1}{\pi} \int_{-\infty}^{\infty} dt' \frac{\Delta}{(t - t'^2 + \Delta^2)} A(t'). \quad (73)$$

The master equation (6) can be then presented in the following form [8]

$$\frac{\partial \bar{\rho}_{nm}(t)}{\partial t} = \sum_m \bar{P}_{nm}(t) [\bar{\rho}_{mm}(t) - \bar{\rho}_{nn}(t)], \quad (74)$$

where

$$\bar{P}_{nm}(t) = 2 \text{Re} \int_0^{\infty} dt' \overline{D_{nm}(t) D_{mn}(t - t')} \exp[i(\omega_{nm} + i\Gamma_{nm})t'] \quad (75)$$

and

$$D_{nm}(t) = \langle \Psi_n | i\hbar \frac{\partial}{\partial t} | \Psi_m \rangle, \quad \Gamma_{nm} = \Delta \dot{\omega}_{nm}. \quad (76)$$

The transition rate (75) is a result of second order perturbation theory in \dot{q} . However, the dimensionless cranking model parameter $\dot{q} |\langle \Psi_n | \partial \hat{H} / \partial q | \Psi_m \rangle| / \hbar \omega_{mn}^2(q)$ is increasing for two neighboring terms and therefore, the perturbation theory criterion can not be fulfilled. We may improve the result (75) by considering the Landau-Zener model [27] of two crossing levels. In the case of the Landau-Zener transitions the probability of a non-adiabatic transition is

$$R^{\text{LZ}}(e, \eta) = \exp\left(-\frac{\pi e^2}{2\eta |\dot{q}|}\right), \quad (77)$$

where e is the gap size and η is the slope of the avoided crossings of two nearest levels. The energy difference ΔE of these levels as a function of q can be represented as

$$\Delta E = (e^2 + \eta^2 q^2)^{1/2}. \quad (78)$$

The highly excited energy levels E_n in Eqs. (74) and (75) exhibit many avoided crossings when the parameter q is varied. We introduce the average transition rate $\langle P^{\text{LZ}} \rangle$ as the probability of transitions per unit time along of the collective path $q(t)$ where the gap sizes e and slopes η are randomly distributed

$$\langle P^{\text{LZ}} \rangle = \dot{q} \int_0^\infty d\eta \int_0^\infty de N(\eta, e) R^{\text{LZ}}(e, \eta). \quad (79)$$

Here $N(\eta, e) d\eta de$ is the number of avoided crossings encountered per unit length and slopes in the interval $[\eta, \eta + d\eta]$ and gap sizes in the interval $[e, e + de]$. The distribution $N(\eta, e)$ has been calculated [23] in the limit where the gap e is small (the asymptotic slope η is only well defined in this limit). Assuming that the matrix elements $\langle \Psi_n | \partial \hat{H} / \partial q | \Psi_m \rangle$ are independently Gaussian distributed, it was shown that

$$N(\eta, e) = \Omega(E) \eta P(e) P'(\eta). \quad (80)$$

The functions $P(e)$ and $P'(\eta)$ are distribution functions of gap sizes and slopes, respectively. In the case of chaotic systems the distributions $P(e)$ and $P'(\eta)$ depend on the spectral statistics [23].

Using the transition rate $\langle P^{\text{LZ}} \rangle$ of (79) we can reduce the master equation (74) into a diffusion equation. Summation of both sides of Eq. (74) over the states n with $E_n < E$ gives,

$$\sum_{n (E_n < E)} \frac{\partial f_n}{\partial t} = - \sum_{n (E_n < E)} \langle P_{nm}^{\text{LZ}} \rangle (f_n - f_m), \quad (81)$$

where $f_n = \bar{\rho}_{nn}$ is the occupation probability. Let us introduce $l(E)$ as the flux of probability from a level with energy less than E to levels with energy greater than E ,

$$l(E) = \sum_{n(E_n < E), m(E_m > E)} \langle P_{nm}^{\text{LZ}} \rangle (f_n - f_m) \quad (82)$$

$$= \int_0^E de_1 \Omega(e_1) \int_E^\infty de_2 \Omega(e_2) \langle P^{\text{L.Z.}}(e_1, e_2) \rangle [f(e_1) - f(e_2)]. \quad (83)$$

Using the cut-off properties of the transition rate (77) we transform the flux $l(E)$ as

$$l(E) = -\Omega(E) \frac{\partial f}{\partial E} D(E) \quad (84)$$

where $D(E)$ is the diffusion coefficient

$$D(E) = \dot{q} \Omega(E) \int_0^\infty de e^2 P(e) \int_0^\infty d\eta \eta P'(\eta) \exp\left(-\frac{\pi e^2}{2\eta |\dot{q}|}\right). \quad (85)$$

Finally, we obtain the basic diffusion equation

$$\Omega(E) \frac{\partial f}{\partial t} = \frac{\partial}{\partial E} \Omega(E) D(E) \frac{\partial f}{\partial E}. \quad (86)$$

This equation gives the Landau-Zener's evolution of the occupation probabilities which is caused by slowly varying set of macroscopic variables $q(t)$.

The distribution functions $P(e)$ and $P'(\eta)$ can be evaluated dependently on the spectral statistics:

(i) For systems with time-reversal invariance (Gaussian orthogonal ensemble)

$$P(e) \approx \frac{\pi^2}{6} \Omega(E) \quad (\text{for small } e), \quad (87)$$

$$P'(\eta) = \frac{\eta}{4\sigma^2} \exp\{-\eta^2/8\sigma^2\}. \quad (88)$$

(ii) For systems without time-reversal invariance (Gaussian unitary ensemble)

$$P(e) \approx \frac{\pi^2}{6} e \Omega^2(E) \quad (\text{for small } e), \quad (89)$$

$$P'(\eta) = \frac{\eta}{2\sqrt{\pi}\sigma^3} \exp\{-\eta^2/4\sigma^2\}. \quad (90)$$

We will calculate the rate of dissipation of energy due to Landau-Zener transitions. Let us introduce the jump probability per unit time into an energy interval $[e, e + de]$ as

$$\mathcal{P}(e) de = \dot{q} \int_0^\infty d\eta N(\eta, e; q) \exp\left[-\frac{\pi e^2}{2|\dot{q}|\eta}\right] de, \quad (91)$$

where $N(\eta, e; q)$ is defined in Eq. (80). The dissipation energy, E_{diss} , is connected with the internal transitions which accompany the macroscopic collective motion. The definition of E_{diss} in terms of the jump probability $P(e)$ depends on the total energy E of the nucleus. We will consider two limiting cases.

(i) $E \approx E_{\text{eq}}$ (motion close to the ground state)

The dissipation rate averaged over the spectral statistics is defined in this case as

$$\left\langle \dot{E}_{\text{diss}} \right\rangle_E = \int_0^{\infty} de \ e \mathcal{P}(e) \quad (92)$$

Using the expressions (91), (80) and (87)-(90) we obtain

$$\text{GOE} : \left\langle \dot{E}_{\text{diss}} \right\rangle_E = \text{const} \cdot \Omega^2(E) \sigma^2(E) \dot{q}^2, \quad (93)$$

$$\text{GUE} : \left\langle \dot{E}_{\text{diss}} \right\rangle_E = \text{const} \cdot \Omega^3(E) \sigma^{5/2}(E) |\dot{q}|^{5/2}. \quad (94)$$

Thus, the friction force is proportional to \dot{q} for the case of GOE and is proportional to $|\dot{q}|^{3/2}$ for GUE statistics. This result is greatly reduced in the case of high excitation energy.

(ii) $E \gg E_{\text{eq}}$ (high excitation energy regime)

The definition of $\langle E_{\text{diss}} \rangle_E$ is different in this case from that of Eq. (92) since transitions with $e < 0$ appear. We have,

$$\left\langle \dot{E}_{\text{diss}} \right\rangle_E = \int_{-\infty}^{\infty} de \ e \mathcal{P}(e) \quad (95)$$

This expression and (91), (80) and (87)-(90) lead to

$$\text{GOE} : \left\langle \dot{E}_{\text{diss}} \right\rangle_E = \text{const} \cdot \Omega(E) \frac{d\Omega(E)}{dE} \sigma^{5/2}(E) |\dot{q}|^{5/2}, \quad (96)$$

$$\text{GUE} : \left\langle \dot{E}_{\text{diss}} \right\rangle_E = \text{const} \cdot \Omega^3(E) \frac{d\Omega(E)}{dE} \sigma^3(E) |\dot{q}|^3. \quad (97)$$

The main feature of this result is the dependence of the dissipation energy on the derivative $d\Omega(E)/dE$ of the level density. This means that time irreversible exchange between the collective and internal degrees of freedom is possible if the phase space volume is increasing with the excitation energy of the system.

IV. NON-MARKOVIAN LANGEVIN-LIKE DYNAMICS OF FERMI-LIQUID DROP

The large amplitude motion of a nucleus can be studied in terms of fluid dynamic approaches which allow us to reduce the problems of the avoided crossings of adiabatic energies $E_n(q)$, see e.g. Eq. (25) for the inertia tensor $B(q)$. In general, the nuclear fluid dynamics is influenced strongly by the Fermi motion of nucleons and is accompanied by the dynamic distortion of the Fermi-surface in momentum space [13, 32]. The presence of the dynamic Fermi-surface distortion gives rise to some important consequences in the nuclear dynamics which are absent in classical liquids. The dynamics of a nuclear Fermi liquid is determined by the pressure tensor instead of the scalar pressure as in a classical liquid. This fact changes the conditions for the propagation of the isoscalar and isovector sound excitations and creates a strong transverse component in the velocity field of the particle flow. Furthermore, because of the Fermi-surface distortion, the scattering of particles on the distorted Fermi-surface becomes possible and the relaxation of collective motion occurs [40]. The equations of motion of nuclear Fermi-liquid take then a non-Markovian form. The memory effects depend here on the relaxation time and provide a connection between both limiting cases of the classical liquid (short relaxation time limit) and the quantum Fermi-liquid (long relaxation time limit). The Markovian dynamics only exist in these two limiting cases.

Under the description of the properties of a drop of quantum Fermi liquid, one can start from the collisional kinetic equation for the distribution function in phase space $f(\mathbf{r}, \mathbf{p}; t)$. Using the standard \mathbf{p} -moment procedure, one can derive the continuity equation for the particle density ρ and Euler-like equation for the velocity field u_ν (for details, see Refs. [12, 13, 33]),

$$\frac{\partial}{\partial t}\rho = -\nabla_\nu(\rho u_\nu), \quad (98)$$

$$m\rho\frac{\partial}{\partial t}u_\nu + m\rho u_\mu\nabla_\mu u_\nu + \nabla_\nu\mathcal{P} + \rho\nabla_\nu\frac{\delta\epsilon_{\text{pot}}}{\delta\rho} = -\nabla_\mu P'_{\nu\mu}, \quad (99)$$

where \mathcal{P} is the isotropic part of the pressure, $P'_{\nu\mu}$ is its anisotropic part caused by the dynamic distortion of Fermi surface and ϵ_{pot} is the potential energy density of inter-particle interaction. The pressure tensor $P'_{\nu\mu}$ is derived by the distribution function in phase space $f(\mathbf{r}, \mathbf{p}; t)$. Considering the dynamic Fermi-surface distortions up to multipolarity $l = 2$ one

can establish [13, 32] the following equation the pressure tensor $P'_{\nu\mu}$

$$\frac{\partial}{\partial t} P'_{\nu\mu} + \mathcal{P} \left(\nabla_\nu u_\mu + \nabla_\mu u_\nu - \frac{2}{3} \delta_{\nu\mu} \nabla_\alpha u_\alpha \right) = I_{\nu\mu} + Y_{\nu\mu}, \quad (100)$$

where $I_{\nu\mu}$ is the second moment of the collision integral $I[\delta f] = -\delta f/\tau$:

$$I_{\nu\mu} = \frac{1}{m} \int \frac{d\mathbf{p}}{(2\pi\hbar)^3} p_\nu p_\mu I[\delta f] \quad (101)$$

and $Y_{\nu\mu}$ gives the contribution from the random force

$$Y_{\nu\mu} = \frac{1}{m} \int \frac{d\mathbf{p}}{(2\pi\hbar)^3} p_\nu p_\mu Y. \quad (102)$$

The equation of motion (98)-(100) are closed with respect to the velocity field u_ν .

For an incompressible and irrotational flow of the nuclear fluid with a sharp surface, the local equation of motion (98)-(100) can be reduced to the equations for the variables $q_i(t)$, $i = \overline{1, N}$ that specify the shape of the nucleus [12]. The continuity equation (98) has to be complemented by the boundary condition on the moving nuclear surface S . Below we will assume that the axially symmetric shape of the nucleus is defined by rotation of the profile function $\rho = \mathcal{L}(z, \{q_i(t)\})$ around the z -axis in the cylindrical coordinates ρ, z, φ . The velocity of the nuclear surface is then given by [34]

$$u_S = \sum_{i=1}^N \bar{u}_i \dot{q}_i, \quad (103)$$

where

$$\bar{u}_i = (\partial \mathcal{L} / \partial q_i) / \Lambda, \quad \Lambda = \sqrt{1 + (\partial \mathcal{L} / \partial z)^2}. \quad (104)$$

The potential of the velocity field takes the form

$$\phi = \sum_{i=1}^N i \bar{\phi}_i \dot{q}_i, \quad (105)$$

where the potential field $\bar{\phi}_i \equiv \bar{\phi}_i(\mathbf{r}, q)$ is determined by the equations of the following Neumann problem

$$\nabla^2 \bar{\phi}_i = 0, \quad (\mathbf{n} \cdot \nabla \bar{\phi}_i)_S = \frac{1}{\Lambda} \frac{\partial \mathcal{L}}{\partial q_i}, \quad (106)$$

where \mathbf{n} is the unit vector which is normal to the nuclear surface. Using Eqs. (98) and (99) with multiplying Eq. (99) by $\nabla_\mu \bar{\phi}_i$ and integrating over \mathbf{r} , one obtains

$$\sum_{j=1}^N [B_{ij}(q) \ddot{q}_j + \sum_{k=1}^N \frac{\partial B_{ij}}{\partial q_k} \dot{q}_j \dot{q}_k + \int_{t_0}^t dt' \exp(\frac{t'-t}{\tau}) \kappa_{ij}(t, t') \dot{q}_j(t')] = -\frac{\partial E_{\text{pot}}(q)}{\partial q_i}. \quad (107)$$

Here $B_{ij}(q)$ is the inertia tensor

$$B_{ij}(q) = m\rho_0 \oint ds \bar{u}_i \bar{\phi}_j \quad (108)$$

and we ignore the random force. The memory kernel $\kappa_{i,j}(t, t')$ in Eq. (107) is given by

$$\kappa_{ij}(t, t') = 2 \int d\mathbf{r} \mathcal{P}(\mathbf{r}, q(t')) \left[\nabla_\nu \nabla_\mu \bar{\phi}_i(\mathbf{r}, q(t)) \right] \left[\nabla_\nu \nabla_\mu \bar{\phi}_j(\mathbf{r}, q(t')) \right]. \quad (109)$$

The potential field $\bar{\phi}_i \equiv \bar{\phi}_i(\mathbf{r}, q)$ are determined by a solution to the Neumann problem (106).

To solve Eq. (107) we will rewrite it as a set of two equations. Namely,

$$\sum_{j=1}^2 [B_{ij}(q) \ddot{q}_j + \sum_{k=1}^2 \frac{\partial B_{ij}}{\partial q_k} \dot{q}_j \dot{q}_k] = -\frac{\partial E_{\text{pot}}(q)}{\partial q_i} + R_i(t, q) \quad (110)$$

and

$$\frac{\partial R_i(t, q)}{\partial t} = -\frac{R_i(t, q)}{\tau} + \sum_{j=1}^2 \kappa_{ij}(q, q) \dot{q}_j \quad \text{at} \quad R_i(t=0, q) = 0, \quad (111)$$

where $q = \{q_1, q_2\} = \{\zeta_0, \zeta_2\}$ and the terms $\sim \dot{q}_i \dot{q}_j$ were omitted in Eq. (111), as the next order corrections. The memory kernel $\kappa_{ij}(q, q)$ is given by

$$\kappa_{ij}(q, q) = \frac{2}{5} m \rho_0 v_F^2 \int d\mathbf{r} (\nabla_\nu \nabla_\mu \bar{\phi}_i(\mathbf{r}, q)) (\nabla_\nu \nabla_\mu \bar{\phi}_j(\mathbf{r}, q)). \quad (112)$$

We will apply this approach to the case of symmetric nuclear fission described, assuming the Lorentz parameterization for the profile function $\mathcal{L}(z)$ in the form of Eq. (35). We have performed numerical calculation for symmetric fission of the nucleus ^{236}U . We solved Eqs. (110) and (111) numerically using the deformation energy $E_{\text{pot}}(q)$ from Refs. [2]. The scission line was derived from the condition of the instability of the nuclear shape with respect to the variations of the neck radius, see Eq. (38). The equations of motion (110) and (111) were solved with the initial conditions corresponding to the saddle point deformation and the initial kinetic energy $E_{\text{kin},0} = 1$ MeV (initial neck velocity $\dot{\zeta}_2 = 0$).

In Figure 7 we show the dependence of the fission trajectory, i.e., the dependence of the neck parameter ζ_2 on the elongation ζ_0 , for the fissioning nucleus ^{236}U for two different values of the relaxation time τ : $\tau = 4 \times 10^{-22}$ s (dashed line) and $\tau = 0 \times 10^{-23}$ s (dotted line). The scission line (dot-dashed line in Figure 7) was obtained as a solution to Eq. (38). We define the scission point as the intersection point of the fission trajectory with the scission line. As can be seen from figure 11 the memory effect hinders slightly the neck formation and leads to a more elongated scission configuration. To illustrate the memory effect on the

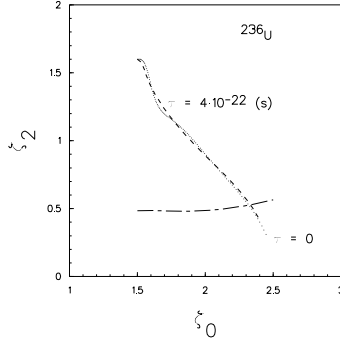


FIG. 7: Trajectories of descent from the saddle point of the nucleus ^{236}U in the ζ_0, ζ_2 plane. Dashed line represents the result of the calculation in presence of the memory effects and dotted line is for the case of Markovian (no memory) motion with the friction forces. We have used the relaxation time $\tau = 4 \times 10^{-22}$ s and the initial kinetic energy $E_{\text{kin}} = 1$ MeV. Dot-dashed line is the scission line derived from the condition (38).

observable values we have evaluated the translation kinetic energy of the fission fragments at infinity, E_{kin} , and the precission Coulomb interaction energy, E_{Coul} . The value of E_{kin} is the sum of the Coulomb interaction energy at scission point, E_{Coul} , and the precission kinetic energy $E_{\text{kin,ps}}$. Namely,

$$E_{\text{kin}} = E_{\text{Coul}} + E_{\text{kin,ps}}. \quad (113)$$

The influence of the memory effects on the fission-fragment kinetic energy, E_{kin} , and the precission Coulomb interaction energy, E_{Coul} , is shown in figure 8. As seen from figure 8, the memory effects are neglected at the short relaxation time regime where the memory integral is transformed into the usual friction force. In the case of the Markovian motion with friction (dashed line), the yield of the potential energy, ΔE_{pot} , at the scission point is transformed into both the precission kinetic energy, $E_{\text{kin,ps}}$, and the time irreversible dissipation energy, E_{dis} , providing $\Delta E_{\text{pot}} = E_{\text{kin,ps}} + E_{\text{dis}}$. In contrast to this case, the non-Markovian motion with the memory effects (solid line) produces an additional time reversible precission energy, $E_{\text{F,ps}}$, caused by the distortion of the Fermi surface. In this case, the energy balance reads

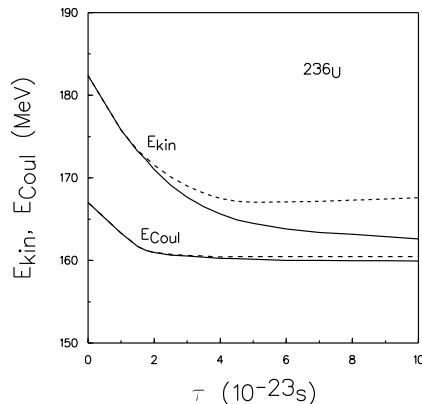


FIG. 8: Fission-fragment kinetic energy, E_{kin} , (curves 1) and the Coulomb repulsive energy at the scission point, E_{Coul} , (curves 2) versus the relaxation time τ for the nucleus ^{236}U . Solid lines represent the result of the calculation in presence of the memory effects and dashed lines are for the case of Markovian (no memory) motion with the friction forces. The initial kinetic energy is $E_{\text{kin},0} = 1 \text{ MeV}$.

$\Delta E_{\text{pot}} = E_{\text{kin,ps}} + E_{\text{dis}} + E_{\text{F,ps}}$. Note that the used parametrization of the fissioning nucleus at the scission point, leads to the prescission Coulomb energy E_{Coul} which is about 5 MeV lower (for ^{236}U) than the Coulomb interaction energy of the scission point shape [35]. Taking into account this fact and using the experimental value of the fission-fragment kinetic energy $E_{\text{kin}}^{\text{exp}} = 168 \text{ MeV}$ [35], one can see from figure 12 that the Markovian motion with friction (dashed line) leads to the overestimate of the fission-fragment kinetic energy E_{kin} . In the case of the non-Markovian motion with the memory effects (solid line), a good agreement with the experimental data is obtained at the relaxation time of about $\tau = 8 \times 10^{-23} \text{ s}$. A small deviation of the prescission Coulomb energy E_{Coul} obtained at the non-Markovian motion (solid line in figure 12) from the one at the Markovian motion (dashed line in figure 12) is caused by the corresponding deviation of both fission trajectories in Figure 8.

In figure 9 we illustrate the memory effect on the saddle-to-scission time t_{sc} . In the case of the non-Markovian motion (solid line), the delay in the descent of the nucleus from the

barrier grows with the relaxation time τ (at $\tau \geq 4 \cdot 10^{-23}$ s). This is mainly due to the hindering action of the elastic force caused by the memory integral. The saddle-to-scission time increases by a factor of about 2 due to the memory effect at the *experimental* value of the relaxation time $\tau = 8 \times 10^{-23}$ s which was derived from the fit of the fission-fragment kinetic energy E_{kin} to the experimental value of $E_{\text{kin}}^{\text{exp}}$ (see above).

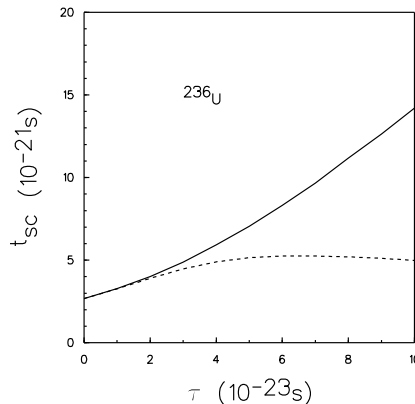


FIG. 9: Dependence upon relaxation time τ of the saddle-to-fission time, t_{sc} , for the descent from the barrier in the case of two-dimension (ζ_0, ζ_2) parametrization for the nucleus ^{236}U . Solid line represents the result of the calculation in presence of the memory effects and dashed line is for the case of Markovian (no memory) motion with the friction forces. The initial kinetic energy is $E_{\text{kin}} = 1$ MeV.

V. SUMMARY

In attempt to understand microscopically the origin for dissipative and fluctuating properties of collective modes of motion in nuclear many-body systems, we have developed an approach, based on the Zwanzig's projection technique (5)–(6).

We have averaged the intrinsic nucleonic dynamics over suitably chosen statistics of the randomly distributed matrix elements (7), measuring the coupling between the intrinsic nu-

cleonic and macroscopic collective $q(t)$ subsystems, and the energy spacings. In assumption of the weak coupling [21], we have derived the diffusion-like equation of motion (10) for the ensemble averaged occupancies of the adiabatic many-body states, describing a process of non-Markovian energy diffusion and that occurs due to quantum-mechanical transitions between the many-body levels. Going beyond the weak-coupling limit [21], we have also studied the energy diffusion process in space of the occupancies of the adiabatic many-body states for Landau-Zener transitions between levels (77), where the diffusive properties essentially depend on quantum statistics of many-body states, see Eqs. (96), (97). It has been demonstrated that under the growing of the averaged density of levels with energy E , the intrinsic nucleonic subsystem parametrically excites, that can, in turn, be interpreted as corresponding dissipation of collective energy due to constancy of the total energy of the nuclear many-body system.

We have shown that memory effects in the diffusion equation (10) is caused by finite spread Γ of the randomly distributed coupling matrix elements (7) and disappears for quite spread distributions, when \hbar/Γ is the shortest time scale in the system. We have demonstrated that a (memory or correlation) time $\tau = \hbar/\Gamma$ defines non-Markovian character of macroscopic collective dynamics (28) and also determines statistical properties of the random force term, incorporated into equations of motion for the collective variables (28), through the fluctuation-dissipation theorem (34).

We have further applied our non-Markovian Langevin approach (28), (34) to the description of descent of the nucleus from the fission barrier. We have showed that the random force accelerate significantly the process of descent from the barrier for both the Markovian and non-Markovian Langevin dynamics, see figure 1. This fact may be explained by the correlation properties (34) of the random force in the non-Markovian Langevin equations.

We have generalized the Kramers' theory of escape rate over parabolic potential barrier (of figure 2) to systems with non-Markovian dynamics (41),(42). The found expression for the escape rate (67) differs from the standard Kramers result (68) by memory-renormalization of the frequency parameter $\tilde{\omega}_{B,\text{sat}}$ (58) at the top of barrier. It has been shown that $\tilde{\omega}_{B,\text{sat}}$ is effectively smaller than the frequency parameter ω_B of the adiabatic barrier, giving rise to slowing down of the thermal diffusion over barrier with the increase of the size τ of memory effects, see figure 3.

We have also studied the non-Markovian diffusion (71), (42) over parabolic barrier in

the presence of weak periodic time perturbation. The mean pre-saddle time was calculated as a function of the frequency ω of the perturbation (see figure 5) and found that the diffusive motion over the barrier may be significantly accelerated at some definite (resonance) frequency ω_{res} , that is defined by the mean time of motion in the absence of perturbation.

By use of p -moments techniques, we have reduced the collisional kinetic equation to the equations of motion for the local values of particle density, velocity field and pressure tensor, see Eqs. (98)–(100). To apply our approach to the nuclear large amplitude motion, we have assumed that the nuclear liquid is incompressible and irrotational. We have derived the velocity field (103)–(106), which depends then on the nuclear shape parameters $q(t)$ due to the boundary condition on the moving nuclear surface. Finally, we have reduced the problem to a macroscopic equation of motion for the shape parameters $q(t)$ (107)–(109). Thus, we consider a change (not necessary small) of the nuclear shape which is accompanied by a small quadrupole distortion of the Fermi surface. The obtained equations of motion for the collective variables $q(t)$ contains the memory integral which is caused by the Fermi-surface distortion and depends on the relaxation time τ .

We have shown that the development of instability near the fission barrier is strongly influenced by the memory effects if the relaxation time τ is large enough. In this case, a drift of the nucleus from the barrier to the scission point is accompanied by characteristic shape oscillations which depend on the relaxation time τ . The shape oscillations appear due to the elastic force induced by the memory integral. The elastic force acts against the adiabatic force $-\partial E_{\text{pot}}(q)/\partial q$ and hinders the motion to the scission point. In contrast to the case of the Markovian motion, the delay in the fission is caused here by the conservative elastic force and not only by the friction force. Due to this fact, the nucleus loses a part of the prescission kinetic energy converting it into the potential energy of the Fermi surface distortion instead of the time-irreversible heating of the nucleus.

The memory effects lead to the decrease of the fission-fragment kinetic energy, E_{kin} , with respect to the one obtained from the Markovian motion with friction, see Figure 7. This is because a significant part of the potential energy at the scission point is collected as the energy of the Fermi surface deformation. Note that the decrease of the fission-fragment kinetic energy due to the memory effects is enhanced in the rare collision regime (at larger relaxation time) while the effect due to friction decreases. An additional source for the decrease of the fission-fragment kinetic energy is caused by the shift of the scission

configuration to that with a larger elongation parameter ζ_0 , in the case of the non-Markovian motion. Due to this fact, the repulsive Coulomb energy of the fission fragments at the scission point in figure 12 decreases with respect to the case of the Markovian motion.

VI. ACKNOWLEDGMENTS

This study was supported in part by the program Support for the development of priority areas of scientific research of the National Academy of Sciences of Ukraine, Grant No. 0120U100434.

VII. REFERENCES

-
- [1] Siemens P J and Jensen A S 1987 *Elements of Nuclei: Many-body Physics with the Strong Interaction* (Reading, MA: Addison–Wesley)
 - [2] Hasse R W and Myers W D 1988 *Geometrical Relationships of Macroscopic Nuclear Physics* (Berlin: Springer)
 - [3] Hofmann H 1997 *Phys. Rep.* **284** 137
 - [4] Boilley D, Suraud E, Abe Y and Ayik S 1993 *Nucl. Phys. A* **556** 67
 - [5] Boilley D, Abe Y, Ayik S and Suraud E 1994 *Z. Phys. A* **349** 119
 - [6] Abe Y, Ayik S, Reinhard P G and Suraud E 1996 *Phys. Rep.* **275** 49
 - [7] Ayik S and Nörenberg W 1982 *Z. Phys. A* **309** 121
 - [8] Kolomietz V M 1995 *Phys.Rev. C* **52** 697
 - [9] Kolomietz V M, Radionov S V and Shlomo S 2006 *Phys. Scr.* **73** 458
 - [10] Kolomietz V M, Åberg S and Radionov S V 2008 *Phys. Rev. C* **77** 04315
 - [11] Kolomietz V M and Radionov S V 2009 *Phys. Rev. C* **80** 024308
 - [12] Kolomietz V M, Radionov S V and Shlomo S 2001 *Phys. Rev. C* **64** 054302
 - [13] Kolomietz V M and Shlomo S 2004 *Phys. Rep.* **390** 133
 - [14] Weidenmüller H A 1980 *Progress in Particle and Nuclear Physics* **3** 49 (Oxford: Pergamon)
 - [15] Bulgac A, Dang G Do, and Kusnezov D 2001 *Physica E* **9** 429; *ibid.* 436

- [16] Grabert H and Weiss U 1984 *Phys. Rev. Lett.* **53** 1787; Ankerhold J, Grabert H, Ingold G-L *et al* 1995 *Phys. Rep.* **168** 115
- [17] Hänggi P, Grabert H, Ingold G L, and Weiss U 1985 *Phys. Rev. Lett.* **55** 761; Hänggi P, Talkner P, and Borkovec M 1990 *Rev. Mod. Phys.* **62** 251
- [18] Rummel C and Ankerhold J 2002 *Euro-Phys. J. B* **29** 105; Rummel C and Hofmann H 2005 *Nucl. Phys. A* **756** 136
- [19] Scheuter F and Hofmann H 1983 *Nucl. Phys. A* **394** 477; Hofmann H, Ingold G L and Thoma M 1993 *Phys. Lett. B* **317** 489
- [20] Zwanzig R 1960 *J. Chem. Phys.* **33** 1338
- [21] Kolomietz V M and Radionov S V 2010 *J. Math. Phys.* **51** 062105
- [22] Gorkov L and Eliashberg G 1965 *Sov. Phys. JETP* **48** 1407
- [23] Wilkinson M 1988 *J. Phys. A* **21** 4021, 1989 *J. Phys. A* **22** 2795
- [24] Brink D M, Neto J and Weidenmüller H A 1979 *Phys. Lett. B* **80** 170
- [25] Zelevinsky V G, Horoi M, and Brown B A 1995 *Phys. Lett. B* **350** 141; 1995 *Phys. Rev. Lett.* **74** 5194
- [26] Pandey A and Mehta M L 1983 *Commun. Math. Phys* **87** 449
- [27] Zener C E 1932 *Proc. R. Soc. A* **137** 696, Landau L D 1932 *Phys. Z. Sow.* **1** 88, **2** 46
- [28] Benzi R, Sutera A and Vulpiani A 1981 *J. Phys. A* **14** L453
- [29] Kramers H A 1940 *Physica* **7** 284
- [30] Kolomietz V M and Radionov S V 2011 *Phys. Rev. E* **84** 051123
- [31] Kolomietz V M and Kondratjev V N 1992 *Z. Phys. A* **344** 125
- [32] Kolomietz V M 1983 *Sov. J. Nucl. Phys.* **37** 325
- [33] Kolomietz V M and Tang H H K 1981 *Phys. Scr.* **24** 915
- [34] Ivanyuk F A, Kolomietz V M and Magner A G 1995 *Phys. Rev. C* **52** 678
- [35] Davies K T R, Managan R A, Nix J R and Sierk A J 1977 *Phys. Rev. C* **16** 1890
- [36] Risken H 1989 *The Fokker-Planck Equation: Methods of Solution and Applications* (Berlin:Springer)
- [37] Adelman S A 1976 *J. Chem. Phys.* **64** 124
- [38] Benzi R, Sutera A and Vulpiani A 1981 *J. Phys. A* **14** L453
- [39] McNamara B, Wiesenfeld K and Roy R 1988 *Phys. Rev. Lett.* **60** 2626
- [40] Abrikosov A A and Khalatnikov I M 1959 *Rep. Prog. Phys.* **22** 329